UNVEILING SPATIAL VARIATION IN SALT AFFECTED SOIL OF GAUTAM BUDDHA NAGAR DISTRICT BASED ON REMOTE SENSING INDICATORS

SHIVANGI S. SOMVANSHI [1], PHOOL KUNWAR[2], WALTER TIMO DE VRIES[3], MAYA KUMARI[4] AND SYED ZUBAIR[5]

[1]*Amity Institute of Environmental Sciences, Amity University, Sector – 125, Noida, India. [ORCID: 0000-0001-9077-6301]*
[2]*Remote Sensing Application Centre – Uttar Pradesh, Lucknow, Uttar Pradesh, India.*
[3]*Department of Civil, Geo and Environmental Engineering, Technische Universitat Munchen, Germany.*
[4]*Amity School of Natural Resources and Sustainable Development, Amity University, Sector-125, Noida, India.*
[5]*Department of Civil Engineering, Amity School of Engineering and Technology, Amity University, Sector-125, Noida, India.*
[*]*Corresponding author e-mail: maya.84s@gmail.com*

Received: 9th January 2020, **Accepted:** 2nd April 2020

ABSTRACT

Salt accumulation within the soil is one of the subtle ecological issues around the world. An integrated of remote sensing with different statistical techniques has indicated accomplishment for creating soil quality forecasting models. The objective of this research was to unveil the degree and location of the salt affected soils as it has a severe effect on the agricultural crop yield of the Gautam Buddha Nagar (GBN) district. To assess spatial variation of the salt-affected soil a simulation model integrating satellite observation data, artificial neural network (ANN) and multiple linear regression (MLR) was used. The statistical correlation amongst ground-truth data and Landsat original bands and band ratios showed that all the bands and ratios showed a non-significant correlation with SAR. While four optical bands and eleven band ratios showed high correlation with all the soil quality parameters. Combining all the remotely sensed variables into models resulted in the finest fit with the R^2 value equal to 0.84, 0.69, 0.59 and 0.85 for EC, pH, ESP and TSS, respectively. The soil quality parameter maps generated using selected models revealed that most of the part of the agricultural land of the study area lies in the range of moderately saline and moderately sodic soil. Further Analytical Hierarchy Process (AHP) was applied to generate overall soil degradation probability map of the district, with respect to salt accumulation. The result revealed that the major portion of the entire agricultural field of the study area lie between low (32.74 %) to moderate (29.53 %) probability zones of salt susceptibility.

Keywords: Soil quality parameters, Landsat OLI & TIRS, Correlation, Artificial Neural Network (ANN), Multiple Linear Regression (MLR), Analytical Hierarchy Process (AHP) and Weighted Index Overlay (WIO)

INTRODUCTION

Sodicity and soil salinity has been a genuine ecological concern worldwide. Soils having electrical conductivity (EC) of the saturation extract higher than four deci-Siemens per meter (dS/m) at 25 °C, Exchangeable Sodium Percentage (ESP) lesser than 15 and pH (soil reaction) lesser than 8.5 are named as saline soils, which means the presence of excess soluble salts such as sulfates, carbonates, & chlorides in the salt solution soil. Differently, soil with a pH greater than 8.5, ESP more than 6 % and a majority of carbonate and sodium bicarbonate are referred to as sodic soil (Richards, 1954). In India, salts in soil grow every year as an outcome of secondary salinization due to human activities such as urbanization and improper irrigation practices. The spatial disposition of excess salt-affected soils over the area is exceedingly delicate and measured by a range of parameters such as parent material, penetrability, water table level, quality of groundwater, topography, irrigation, rainfall, drainage and humidity (Douaik *et. al.,* 2004). Around 7 million hectares area of India including the states of West Bengal, Uttar Pradesh, Gujarat, Punjab, Rajasthan, Maharashtra, Delhi, Haryana, Tamil Nadu, Kerala and Orissa are facing soil problems due to salt accumulation out of which about 2.8 million hectares of salt containing soils are present within the Indo-Gangetic alluvial plain (Abrol & Bhumbla, 1971).

The addition of salts in agricultural lands caused by irrigation and other escalated agricultural pursuits, deteriorates cropland producing the degeneration in the efficiency of crops and thus favoring the decline in agricultural yields (Patel *et al*., 2009; Akramkhanov, 2011). The accumulation of salt in the soil is a continuous and changing process, which requires to be observed continuously in order to have the most recent knowledge of their extent, level of graveness, nature, spatial dispersal and expanse (Azabdaftari & Sunar, 2016). Understanding when, where and how salts impact may occur, is very critical to the sustainable advancement of any agricultural land framework. Ground-based measurement of EC and pH is usually recognized as the highest efficient technique for measurement of the quantity of salt-affected soils (Norman *et. al.*, 1989). Traditional methods of measuring salt in soil by collecting and analyzing samples in the laboratory are expensive, tedious and need extensive manpower for surveying and mapping of land. The dynamic nature of the salt-affected soil in space and time makes it more challenging to use traditional techniques for a large area (IDNP, 2003). For monitoring such kind of dynamic processes, remote sensed data has great potential.

Over a few decades, remote sensing information has been extensively used as a cost-effective method to map salt-affected soil, either directly or indirectly, in a real-time at different scales (Metternicht & Zinck, 2008). Interesting studies have been done for salt recognition in soil using optical multispectral, microwave and thermal remote sensing techniques synergistically in recent years. High precision sensors onboard various satellites are quite helpful in identifying and observing the saline and sodic soils. Multi-spectral data such as SPOT, LANDSAT, IKONOS, IRS, EO-1 & Terra-ASTER with resolution ranging from average to high along with hyperspectral sensors can be utilized for detecting salts in the soil. Kant *et. al.* (1997) effectively delineated, mapped and digitally classified salt affected and waterlogged zones of India using bands 3, 4, 5 and 7 of Landsat TM image with an accuracy of about ninety six percent. Those sensors can only scan the upper surface of dirt, whereas the whole profile of soil is affected and should be inspected. This restraint calls for the requirement of utilizing some additional techniques and data, in collaboration with remote sensing (Farifteh, 2006).

It creates the impression that the utilization of statistical tools and spectral transformation as often as possible have a great outcome for upgrading the derivation of soil-related

information from spectral bands. Spatial modeling, which is the use of numerical mathematical statements to simulate real phenomenon and processes, has followed several methodologies for evaluating and predicting salt problems in soil (salinity or sodicity). Several approaches have been used for spatial modelling till date, few of them are Artificial Neural Network (Akramkhanov & Vlek, 2012), Regression Tree (Mehrjardi *et. al*., 2014), Fuzzy Logic, Generalized Bayesian Analysis (Douaik *et. al*., 2004), Geostatistics (eg. Kriging, Cokriging, Regression Kriging) (Tajgardan *et. al*., 2010) and Statistical Analysis (regression, ordinary least square) (Judkins & Myint , 2012). Bouaziz *et al*. in 2011 stated a reasonable relation between spectral indices and electrical conductivity using the linear spectral unmixing (LSU) method to enhance the estimation of salt-affected soil using MODIS data. It was also revealed that the application of LSU improves the correlation. Bannari *et al* in 2008 proposed that SSSI (Soils Salinity and Sodicity Indices) making use of EO-1 ALI 9 and spectral bands (ten) gives significantlybestcorrelation with the ground truth data of electrical conductivity and proved efficient to simulate various spatial distribution categories of low and moderately salt-affected soil.A multiple linear regression model grounded on various digital image enhancement techniques have also been broadly used to forecast salt concentration in soil and to enhance the characterized variability of salinity or sodicity. Jian-li et al. in 2011 used a Landsat ETM+ image to focus the main variables to be put in use for extraction and classification of salinised soils using decision tree methodology of principal component analysis (PCA). Afework in 2009 constructed a trustworthy linear regression model to simulate salt-affected soil in the sugarcane farms of Ethiopia by correlating NDSI to electrical conductivity. Janik *et al*. in 2009 stated that forecasting variety of physical and chemical characteristics of soil from MIR spectra using PLSR and neural networks combination. Cozzolino and Moron in 2003 utilized modified partial least squares (MPLS) regression and first derivative transformation of the reciprocal reflectance to inspect soil samples for sand, silt, clay, Cu, Ca, Mg, K, and Fe. Principally, PLSR is the most frequently assessed spectral treatment technique on the statistical basis for soil studies. Lately, Judkins and Myint in 2012 invented that Landsat band 7, Tasseled Cap 3 and 5 and Transformed Normalized Difference Vegetation Index (TNDVI) resulted from TCT, showed better correlation with the spatial distribution in soil salinity. Integrating these spectral variables into a regression model (MLR) assisted them to map and simulate spatial distribution levels of salt-affected soil efficiently (Allbed *et. al.*, 2014).

Poor crop productivity in salt-affected environment in the selected study area (GBN district of Uttar Pradesh) is due to insufficient and untimely canal supply to agricultural land and inefficient field water management practices. This could further degrade due to inadequate maintenance of canal network, ongoing secondary soil salinization and waterlogging, worsening of groundwater quality. Large patches of low productivity in irrigation commands are occurring due to waterlogging and salt-affected soil. Therefore, the primary aims of conducting this research are: (i) to interpret and understand the spectral reflectance attributes of salt affected soils in Gautam Buddha Nagar district, (ii) to investigate the capability of Landsat imagery to spot and map the salts in soil over the area of interest, (iii) to assess interrelationship between on-field measurements and data procured from Landsat imagery, and (iv)to develop spatial dataset classified with very high, high, moderate, low and least degradation probability zones. We address these questions in the following sequence. We first describe the characteristics of the study area and which data are gathered in this area. Then, we explain how and with which methods we analyze the data, followed by a presentation of the results. We conclude by addressing the main research questions and formulating a set of recommendations how to continue this study.

STUDY AREA

This study presents an approach based on input feature selection (with ANN) and empirical modelling fed with different Landsat 8 OLI spectral band ratios, calibrated using soil salinity data collected in-situ. The location where we collected such data is Gautam Buddha Nagar (GBN) district of NCR region. GBN district falls in Yamuna sub-basin at latitude $28024^{0}14.731$" N and longitude of $77032^{0}33.870$" E (Figure 1). The district spans over an area of around 1442 square kms. and is at an elevation of around 200 meters above MSL. The primary water sources include the groundwater aquifers and few surface water canals that are scattered across the region.

Fig. 1: Location map of study area

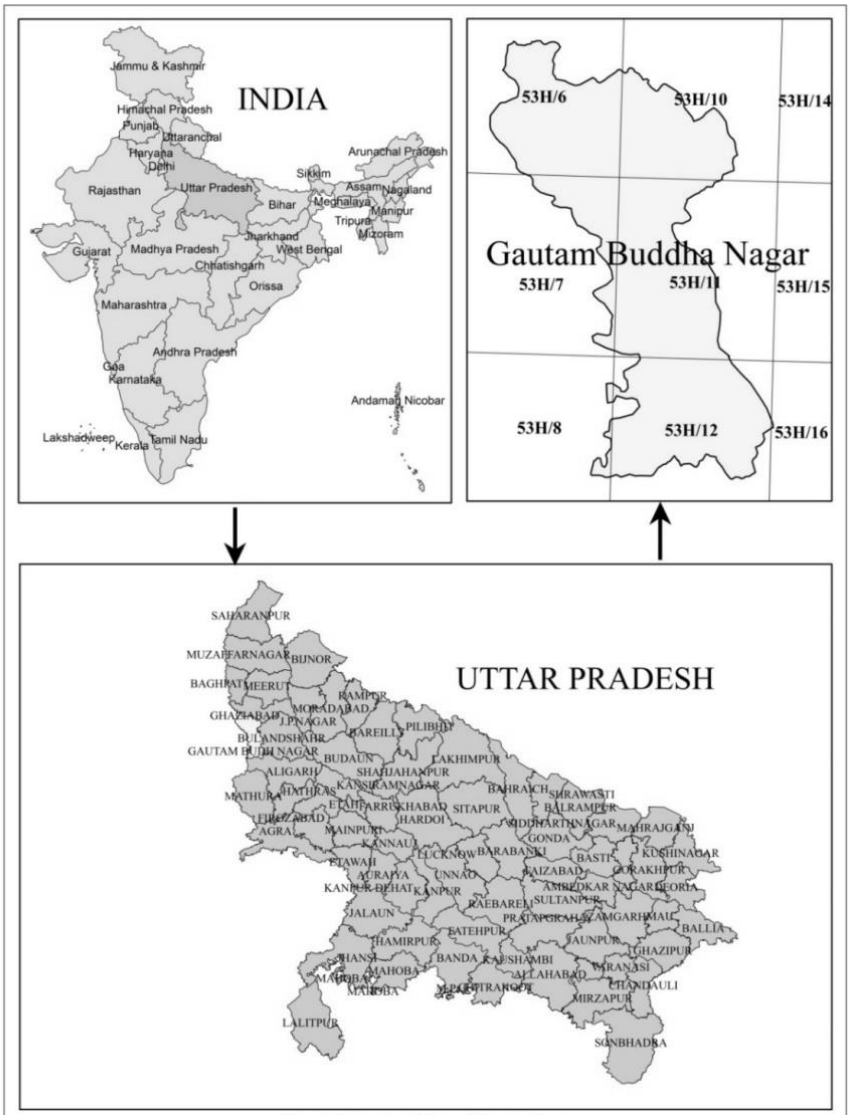

A large portion of the district falls in upper Ganga canal command. Eastern part of the district has a good network of canals. The irrigation of the district is basically met by means of minor irrigation structures such as tube wells and dug wells. The district is known for its sub-humid weather pattern along-with scorching summers and exhilarating cold winters. The yearly average precipitation of the region is round about 600 mm. The absolute ambient temperature goes over 32 °C during the summer season and during winters the average mean temperature is approximate 14 °C. The soil ranges from pure sand to stiff clays and including all combination of the two extreme litho units. The major field crops fertilized are wheat, rice, sugarcane, maize, barley, mustard, pigeon pea.

DATA COLLECTION

Field Sampling

Sampling sites were selected based on the division of the district and varying extent of settlements. Gautam Buddha Nagar district is divided into 4 blocks Bisrakh, Dadri, Dankaur, and Jewar. Out of these blocks, Bisrakh is completely urbanized, remaining three are covered with agricultural fields. Composite soil sampling was performed twice following the sampling procedure of Bouaziz et al. (Bouaziz *et. al.*, 2011). Firstly, during February 2014 for the development of the model and secondly, during February 2016 for the validation of the model. Soil samples were collected from over 50 locations covering 20 villages of three blocks (Dadri, Dankaur, and Jewar) of the district. The 50 sampling locations of the field samples were recorded on a Global Positioning System (GPS) unit, and a GIS map was generated (Figure 2). Each composite sample of soil consisted of four core sub-specimens that were collected at a span of20 m north, south, east and west of the center sampling point. The sub-specimens were gathered from the surface horizon (0–20 cm) with a hand auger (10 cm diameter) which were grinded and blended with each other to form one sample. Since the aim of this research was to develop a correlation between soil quality parameters (EC, pH, TSS, ESP and SAR) and satellite based spectral bands and extrapolate point data to produce a soil degradation probability map of the study area, direct measurements of soil salinity and sodicity were carried out by taking the measurements of EC, pH, TSS, SAR and ESP in the soil saturation extracts in the laboratory, as narrated by Richards (Richards, 1954).The formula used for the calculation of TSS, SAR and ESP is as mentioned below:

$$\text{TSS (mg/l)} = \text{EC (dS/m)} \times 640 \quad \text{..... (i)}$$

$$\text{SAR} = [\text{Na}] / \sqrt{(1/2\ ([\text{Ca}] + [\text{Mg}]))} \quad \text{..... (ii)}$$

$$\text{ESP} = \text{Exchangeable } \{(\text{Na})/(\text{Ca} + \text{Mg} + \text{K} + \text{Na})\} \times 100 \quad \text{..... (iii)}$$

Although ESP and SAR cannot be determined directly from a soil saturation extract, the other variables used for the calculation of ESP and SAR i.e. sodium, calcium, magnesium and potassium can be calculated using a saturated soil paste.

Fig. 2: Distribution of sample points over the study area

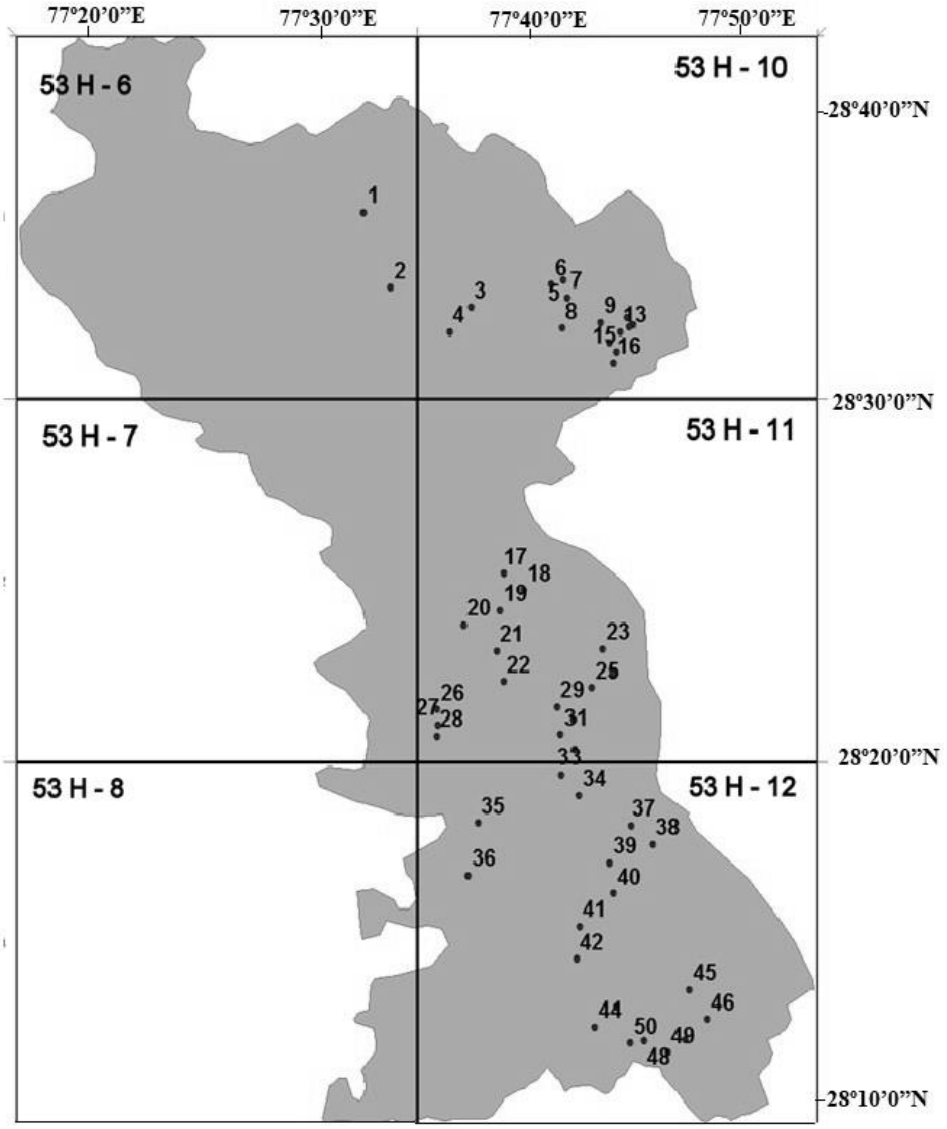

Satellite Data

Satellite data of Landsat-8 (OLI & TIRS) of Path – 146 and Row - 40 were obtained, for the preparation of the models of salt-affected soils. Satellite images employed in this research were obtained near the actual soil sampling date on 9th February 2014 and 2nd March 2016 (Table 1). Although comparing just two values may be considered a limitation for longitudinal change and transformation studies, this specific study primarily aimed at finding a meaningful method to unravel variation, and not to predict long term changes. Firstly, the pre-processing methods such as radiometric and atmospheric corrections should be applied to multi-temporal Landsat images. The un-stripping of Landsat satellite data was carried out

as a radiometric rectification. Then, atmospheric rectification was applied in order to lower the effect of various atmospheric parameters. Such corrections are highly recommended in the studies, where in a correlation between on-field measurements and spectral reflectance values are required (Selch, 2012). Reflectance calibration is applied by deriving the reflectance value from the DN and computing the top of atmosphere reflectance (TOA). In short, the satellite data enable a pixel based spatial modelling using reflectance values of the satellite image using ERDAS IMAGINE 14 software Change in the characteristics of the soil will definitely affect the reflectance value of the pixel. Therefore, the accuracy of the model depends on its ability to detect this variation in the reflectance value of the satellite data and predicting soil quality irrespective of the time and years.

Table 1: Satellite Data Used for the Study

Satellites	Acquisition Date	Sensor	Spatial Resolution	Projection
Landsat 8	02/03/2016	OLI-TIRS	30 m	WG84 UTM Zone 44N
Landsat 8	09/02/2014	OLI-TIRS	30m	WG84 UTM Zone 44N

DATA ANALYSIS

Image Processing (Spectral Enhancement)

Since the adoption of satellite-based recording of spectral radiance of ground objects in visible and near-infrared bands became possible, various indices have been developed based on the certain combinations (sum, difference, ratio, linear-additional) of bands (Somvanshi *et. al.*, 2017). These indices enable the identification and monitoring of temporal variations in objects. The variety of indices has an additional advantage that they can reduce the effects of external factors, such as solar irradiance, atmospheric influence etc. (Girard & Girard, 2003). Two salinity based index (Normalized Differential Salinity Index and Salinity Index) and one vegetation based index (Normalized Differential Vegetation Index) as shown in table no. 2, were used to create enhanced images for the modeling of salt-affected soil using ERDAS IMAGINE 14 software. These indices were shortlisted because of their very high substantial relation with EC and pH. Due to absorption in the visible region and high reflectance in the NIR range of the electromagnetic spectrum, NDVI has been mostly employed to map the salt affected soils by monitoring vegetative cover (Fernandez-Buces *et. al.*, 2006; Elnaggar & Noller, 2009; Jabbar & Chen, 2008). Khan *et. al.* in 2005 also revealed that NDSI resulted in the most acceptable outcomes in recognizing various salt classes compared to other salinity indices in case of cropped land.

Table 2: List of Spectral Indices Used in the Study

S. No.	Vegetation Indices	Formula
1	Normalized Differential Salinity Index (NDSI)	(R – NIR) / (R + NIR)
2	Salinity Index (SI) Tripathi*et al.*(1997)	SI = R/NIR X 100
3	Normalized Differential Vegetation Index (NDVI)	(NIR – R) / (NIR + R)

Band Ratio is the quotient between the reflectance of separate bands of the electromagnetic spectrum. Band ratioing is highly effective in enlightening concealed details when there is an inverse association amongst two spectral responses to the same biophysical phenomenon. Absorption of red wavelength (R) by chlorophyll contents of the leaves and strong reflection

of infrared (IR) wavelength by mesophyll cells of leaves, resulting in deviating different spectrum response from healthy green vegetation in red and NIR radiation. Therefore, the reflectance of the ratio of infrared band to red band (IR/R) of the actively growing plant will be high. On the other hand, the non-vegetated surface which includes water, man-made features, bare soil, stressed vegetation and dead vegetation will not show this specific spectral response and thus the reflectance value of the ratio would be less. Thus, the infrared to red band proportion can be used to measure photosynthetic activity and biomass within a pixel. The IR/R ratio is only one of many measures of vegetation vigor and abundance (Campbell, 2002). Knipling (1970) applied ratio between visible and near-infrared radiation on the physiologically based reflectance of vegetation. Since the time satellite recording of spectral radiance of ground objects in visible and near-infrared bands became possible, many others have developed various band ratios based on the certain combinations (sum, difference, ratio, linear-additional) of bands. These ratios are used to identify and monitor the temporal variation of water bodies. Band ratios which have been used in the present study for the modeling of salt-affected soil are B2/B3, B2/B4, B2/B5, B2/B6, B2/B8, B3/B2, B3/B4, B3/B5, B3/B6, B3/B8, B4/B2, B4/B3, B4/B5, B4/B6, B4/B8, B5/B2, B5/B3, B5/B4, B5/B6, B5/B8, B6/B2, B6/B3 , B6/B4, B6/B5, B6/B8, B8/B2 ,B8/B3, B8/B4 ,B8/B5 , and B8/B6 (Band 2= Blue, Band 3=Green, Band 4=Red, Band 5=NIR, Band 6=SWIR–1, Band 7=SWIR–2 and Band 8=Panchromatic Band). These ratios were developed using the modular of the ERDAS IMAGINE 14 software (Somvanshi *et. al.*, 2012). All the images produced after spectral enhancement was used for the development of models for monitoring and predicting salt-affected soil over the study area.

MODEL GENERATION

The statistical analysis used SPSS 20 software. Pearson correlation, artificial neural network (ANN) and multiple linear regression (MLR) were put in use to calculate the association between the soil parameters (dependent variables) and pixel values of the satellite image (independent variables). Pearson correlation analysis between Landsat-8 (OLI &TIRS) bands, band ratios and spectral indices with soil quality parameters was performed to disclose the association amongst these variables and evaluate their effectiveness in forecasting salt-affected dirt. This statistical tool assisted in exclusion of insignificant independent variables; only the ones having a high correlation with dependent variables were selected. The highly correlated variables were then subjected to ANN modeling. ANN is logically encouraged computer programs envisioned to innervate the pattern in which the human mind computes the information and therefore, it is categorized in the artificial intelligence category of the neural network models. ANN Model was run on the data using Multi-Layer Perceptron (MLP) plugin of SPSS-20 software. Soil quality parameters were given as dependent variable and all other spectral values were given as independent variables. The model was run recurrently for the chosen independent variables for different activation functions and numbers of hidden layers until an acceptable R square value was obtained. The model gave a ranking of the independent variables for forecasting different soil quality parameters respectively.

Further, MLR models were put in use to measure the associations amongst the various soil attributes and shortlisted bands and band ratios of the satellite data. The model was applied on different soil quality attributes and spectral variables on the basis of the normalized importance graph achieved through ANN. MLR model was carried out repeatedly using different combinations of five spectral variables, in accordance with resulted normalized

importance graph through ANN. The coefficients of chosen variables were used to generate ten regression equations for prediction of each soil quality parameter respectively. After comparing the regression coefficients (R^2), the standard error of the mean Y estimate (SE(Y)), and P - value at 95 % confidence level, the best-suited regression model was selected for developing unique class simulated maps for each soil quality parameter.

Model Validation

The developed regression models on the satellite data of 2014 were validated and quantified using the field collected ground truth data and satellite image of 2016, to certify that they not only applicable on a specific data set but also generated precise results on several data sets. In order to validate the models, two quantitative criteria R^2 and RMSE, were calculated between the computed and forecasted values. R^2 values specify the integrity of the statistical linear relationship between two values, and RMSE indicates absolute estimation errors (Moriasi *et. al.*, 2007). Further, normal probability plots, scatter plots and Shapiro–Wilk tests (W) were performed using SPSS 20 to evaluate the normal distribution of the residuals. If the W test is significant ($p < 0.05$) or greatly significant ($p < 0.001$) then the distribution is non-normal (Field *et. al.*, 2012).

Analytical Hierarchy Process (AHP)

Finally, all the simulated maps generated using regression models along with maps generated through indices were subjected to AHP. AHP is a technique which enables the combination of weighting various criteria and of solving problems which need to be addressed from using multiple dimensions. We need AHP to reveal salt accumulation and use this to generate the overall soil degradation probability map. AHP was put to use to allocate the weights to all the six criteria (pH, EC, TSS, ESP, NDVI, and NDSI). AHP is an effective tool for linking qualitative and quantitative elements through expert's opinion and has a capability to evaluate the discrepancies in judgments, hence ensure accuracy of the results. The basis of AHP lies on the creation of a chain of 'pairwise comparison' matrices which compares all the criteria with one another. In the present study, it was done to estimate the weight of each of the criteria which states the importance of the criteria in contributing to the whole aim. This method was carried in three significant steps: (i) the pairwise comparison matrix generation; (ii) the criterion weights computation; and (iii) the consistency ratio estimation. Easy AHP module of QGIS 2.18 was used for the implementation of each of these steps in this study. The AHP process is as shown in Figure 3.

Criteria and alternatives are allocated weights on a 9 point ordinal scale by virtue of pairwise comparison amongst them, as mentioned in table 3given by Saaty (1977). The pairwise comparison matrix was utilized for the computation of weights in terms of eigenvectors (Saaty, 1980, 2000; Ramanathan, 2001). The six criteria were compared pairwise and weights were assigned to each of the criteria on a scale, spanning from one to nine depending on their comparative significance with respect to one another in having an adverse influence on the environment. The outcome of this assessment is displayed in the format of a pairwise comparison matrix (Table 4).

Fig. 3: AHP Process

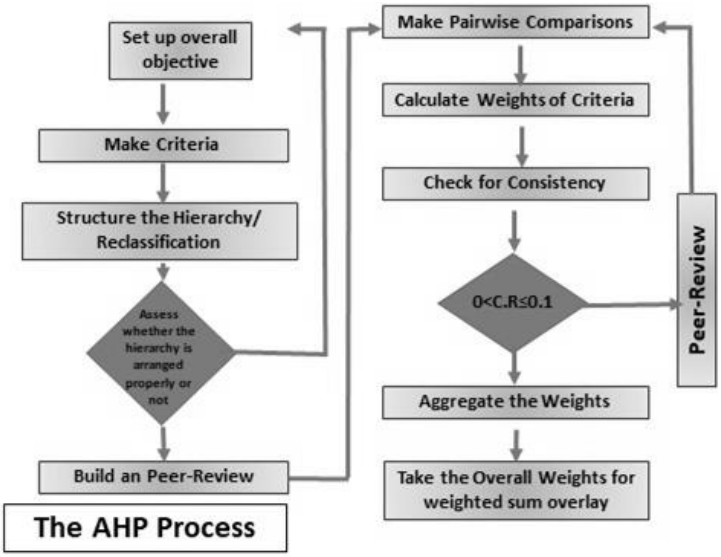

Depending on different data input, the factors can be allocated weights. The calculated factor weights can be subjective sometimes, hence to dodge such a case, the steadiness of the comparison matrix is specified using the consistency ratio (CR). CR is stated as the ratio between the consistency index (CI) and the random index (RI). Random Index is the consistency index of a randomly created pair-wise comparison matrix. Random Index was developed by Saaty (1980, 2000), based on many random samples taken. CI is defined in equation (iv).

$$CI = \lambda_{max} - n / n - 1 \ldots\ldots\ldots \text{(iv)}$$

here,

λ_{max} = biggest eigenvalue of the matrix and n = number of factors (here, n = 6). Saaty proposed that if this proportion is more than 0.1, the set of judgments may be overly inconsistent to be dependable. If the value of CR equals to zero, this implies that the judgments are flawlessly consistent. Further, with the help of a pairwise matrix weighted linear combination (WLC) was awarded to different criteria.

Table 3: Definition of Numerical Scales for Pair-Wise Comparison (Saaty 1977)

Preference/ordinal scale	Degree of preference	Remarks
1	Equally	Factors inherit equal contribution
3	Moderately	One factor moderately favoured over other
5	Strongly	Judgment strongly favour one over other
7	Very strongly	One factor very strongly favoured over other
9	Extremely	One factor favoured over others in highest
2, 4, 6, 8	Intermediate	Compensation between weights 1,3,5,7 and 9
Reciprocals	Opposite	Refers inverse comparison

Table 4: Pair-wise Matrix

	NDSI	TSS	EC	NDVI	ESP	pH
NDSI	1	3.0	1.0	1.0	3.0	3.0
TSS	0.333	1	1.0	3.0	3.0	2.0
EC	1.0	1.0	1	1.0	2.0	1.0
NDVI	1.0	0.333	1.0	1	3.0	1.0
ESP	0.333	0.333	0.5	0.333	1	2.0
pH	0.333	0.5	1.0	1.0	0.5	1

To identify and map the soil degradation probability zones with respect to salt accumulation, various maps (EC, pH, TSS, ESP, NDVI and NDSI) generated were integrated into ArcGIS 10.5. The weights calculated through AHP were assigned to each criteria. Attribute values were scored using a 1 to 5 scale, where 1 is the least susceptible and five being the highest susceptible.

RESULTS

Correlation Matrix

Correlation matrices were produced for Landsat 8 (OLI & TIRS) bands (B2, B3, B4, B5, B6, B7 and B8), band ratios (B1, B2, B3, B4, B5, B6, B7, B8), band ratios (B2/B3, B2/B4, B2/B5, B2/B6, B2/B8, B3/B2, B3/B4, B3/B5, B3/B6, B3/B8, B4/B2, B4/B3, B4/B5, B4/B6, B4/B8, B5/B2, B5/B3, B5/B4, B5/B6, B5/B8, B6/B2, B6/B3, B6/B4, B6/B5, B6/B8, B8/B2, B8/B3, B8/B4, B8/B5, and B8/B6), spectral indices (NDVI and NDSI) and soil quality parameters (pH, EC, SAR, ESP and TSS).

Table 5: Descriptive Statistics of Soil Quality Parameters

Soil Quality Parameters → Descriptive Statistics ↓	EC	pH	ESP	TSS	SAR
Mean	6.311	9.031	8.975	4039.040	0.371
Max	16.000	10.45	14.230	10240.000	0.980
Min	2.300	8.000	6.100	1472.000	0.010
SD	3.407	0.516	2.065	2180.406	0.241
CV (%)	54	5	23	54	65

The main descriptive statistics for all soil quality parameters are mentioned in Table 5. As per the classification of soil salinity by the Food & Agriculture Organization (FAO), EC of the samples of the region of interest varies from highly saline (>16 dS/m) to moderately-saline (2-4 dS/m). A 54 % Coefficient of Variation (CV) confirms the moderate changes in the EC values across the study region. On the other hand, more than 50 % of the total samples were categorized as strongly sodic due to high pH. Although the changes in the pH values over the study areas are very low. Total dissolved solids (TDS) in the soil samples were ranged between 1472 mg/l to 10240 mg/l. Sodium adsorption ratio (SAR) varied from 0.01 to 0.98.

Statistical correlation between ground truth data (EC, pH, ESP, SAR & TSS) and Landsat original bands and band ratios showed that all the bands and ratios showed a non-significant correlation with SAR. Four original bands (B2, B3, B4 and B7) & eleven band ratios (B2/B3,

B2/B4, B2/B5, B3/B2, B3/B4, B3/B5, B4/B2, B4/B3, B4/B5, B6/B5, and B8/B5) showed high correlation with all the soil quality parameters except SAR (Table 6).

Table 6: Correlation Matrix between Soil Quality Parameters and Spectral Variables

Soil Quality Parameters → Spectral Variables ↓	EC	pH	ESP	TSS	SAR
B1	0.489608	0.530015	0.454299	0.489608	0.178842
B2	0.700419	0.68237	0.613012	0.700419	0.305047
B3	0.762493	0.700348	0.64491	0.762493	0.373985
B4	0.831199	0.747272	0.693068	0.831199	0.41491
B5	-0.47124	-0.51386	-0.48172	-0.47124	-0.2805
B6	0.63671	0.582573	0.536913	0.63671	0.349028
B7	0.808919	0.730462	0.666938	0.808919	0.393227
B8	0.704805	0.638486	0.579223	0.704805	0.367305
B2/B3	-0.78412	-0.65641	-0.62249	-0.78412	-0.44194
B2/B4	-0.86525	-0.77108	-0.71071	-0.86525	-0.43349
B2/B5	0.708908	0.725105	0.671349	0.708908	0.363758
B2/B6	-0.48935	-0.44236	-0.43577	-0.48935	-0.27372
B2/B8	-0.65649	-0.58872	-0.54188	-0.65649	-0.39317
B3/B2	0.785029	0.655532	0.624082	0.785029	0.445828
B3/B4	-0.86493	-0.78723	-0.71905	-0.86493	-0.41425
B3/B5	0.808386	0.788761	0.733964	0.808386	0.427314
B3/B6	-0.34584	-0.32305	-0.32446	-0.34584	-0.18701
B3/B8	-0.49368	-0.48668	-0.43692	-0.49368	-0.33066
B4/B2	0.875151	0.764136	0.712246	0.875151	0.451868
B4/B3	0.877912	0.784886	0.722922	0.877912	0.429113
B4/B5	0.867193	0.812392	0.756213	0.867193	0.450622
B4/B6	0.162157	0.137494	0.088017	0.162157	0.070947
B4/B8	0.41429	0.289283	0.280506	0.41429	0.096287
B5/B2	-0.67537	-0.70621	-0.64551	-0.67537	-0.34022
B5/B3	-0.75141	-0.75399	-0.69447	-0.75141	-0.38626
B5/B4	-0.78814	-0.77518	-0.70941	-0.78814	-0.39139
B5/B6	-0.64406	-0.63225	-0.60467	-0.64406	-0.37072
B5/B8	-0.64926	-0.61407	-0.59079	-0.64926	-0.34261
B6/B2	0.499962	0.429441	0.423055	0.499962	0.272057
B6/B3	0.35398	0.316532	0.314205	0.35398	0.184681
B6/B4	-0.14476	-0.11939	-0.07779	-0.14476	-0.06391

B6/B5	0.675274	0.629408	0.602603	0.675274	0.379737
B6/B8	0.389952	0.328635	0.345504	0.389952	0.241116
B8/B2	0.649124	0.582808	0.536927	0.649124	0.405632
B8/B3	0.462741	0.460777	0.415523	0.462741	0.328391
B8/B5	0.69326	0.645929	0.610002	0.69326	0.371842
B8/B6	-0.36362	-0.31771	-0.32268	-0.36362	-0.2292
NDVI	-0.84225	-0.80235	-0.74149	-0.84225	-0.42836
NDSI	0.842246	0.802352	0.741494	0.842246	0.428361
SI	0.867192	0.812392	0.75621	0.867192	0.450622

Furthermore, good correlation results were found between indices and soil parameters with the R^2 values more than 0.8 for almost all the parameters except SAR. Fernandez-Buces *et al*., 2005 stated a substantial correlation between NDVI, SAR, & EC. Later, Pérez González *et al*. in 2006 have tried to find out the relation between the spectral values of NDVI of halophytic vegetation with the spatial variability of the physical and chemical characteristics of an area to recognize saline hydromorphic soils. Their outcomes demonstrated that NDVI is highly efficient in identifying vegetation and relating it to the salt-affected soil. Also, Bannari *et al*. in 2008 have stated that salt stress could be forecasted by employing NDVI due to decline in vegetation cover. Fan *et al*. (2012) discovered that NDVI values had a noteworthy negative interrelation with salt-affected soil, whereas, soil salinity indices exhibited high positive correlations with EC and pH.

Artificial Neural Network (ANN) and Multiple Linear Regression (MLR)

The ANN model was run on the ground truth and spectral variable data using Multi-Layer Perceptron (MLP) in SPSS-20 software. Based on normalized importance (Figure 5) and correlation coefficients B2, B4, B7, B8, B2/B4, B3/B4, B3/B5, B4/B2, B4/B3, B4/B5, B5/B8, B8/B5, B3/B2, and B6/B5 were shortlisted as most significant independent variables for the prediction of EC. Similarly, B3, B4, B4/B3, B2/B5, B2, B4/B5, B8/B5, B5/B6, B3/B5, B4/B2, B3/B4, B5/B4, B5/B3 and B2/B4 were shortlisted for pH; B2/B3, B3, B4, B5/B2, B4/B3, B5/B3, B5/B4, B8/B5, B3/B2, B2/B5, B2/B4, B3/B4, B3/B5, B4/B2 and B4/B5 were shortlisted for ESP and finally, B2, B4, B6, B7, B8, B8/B2, B2/B5, B6/B5, B2/B8, B5/B8, B4/B3, B4/B2, B4/B5, B3/B4, B2/B4, B3/B5 and B5/B4 were shortlisted for the prediction of TSS. Shortlisted bands and band ratios were subjected to MLR.

Stepwise regression was applied to ascertain the variables that satisfactorily described the majority of the variability of the dependent variables, which were EC, pH, ESP, and TSS. Ten models each were developed for individual parameters, respectively, as shown in Table No. 7. Once all the developed regression models were assessed, models with (i) a high R^2, denoting a strong linear relationship, (ii) low standard errors of the model's variables and (iii) not many variables with a *p*-value of less than 0.05 were chosen for the assessment using the testing data.

Fig. 5: Normalized importance graph for (a) EC (b) pH (c) ESP and (d) TSS

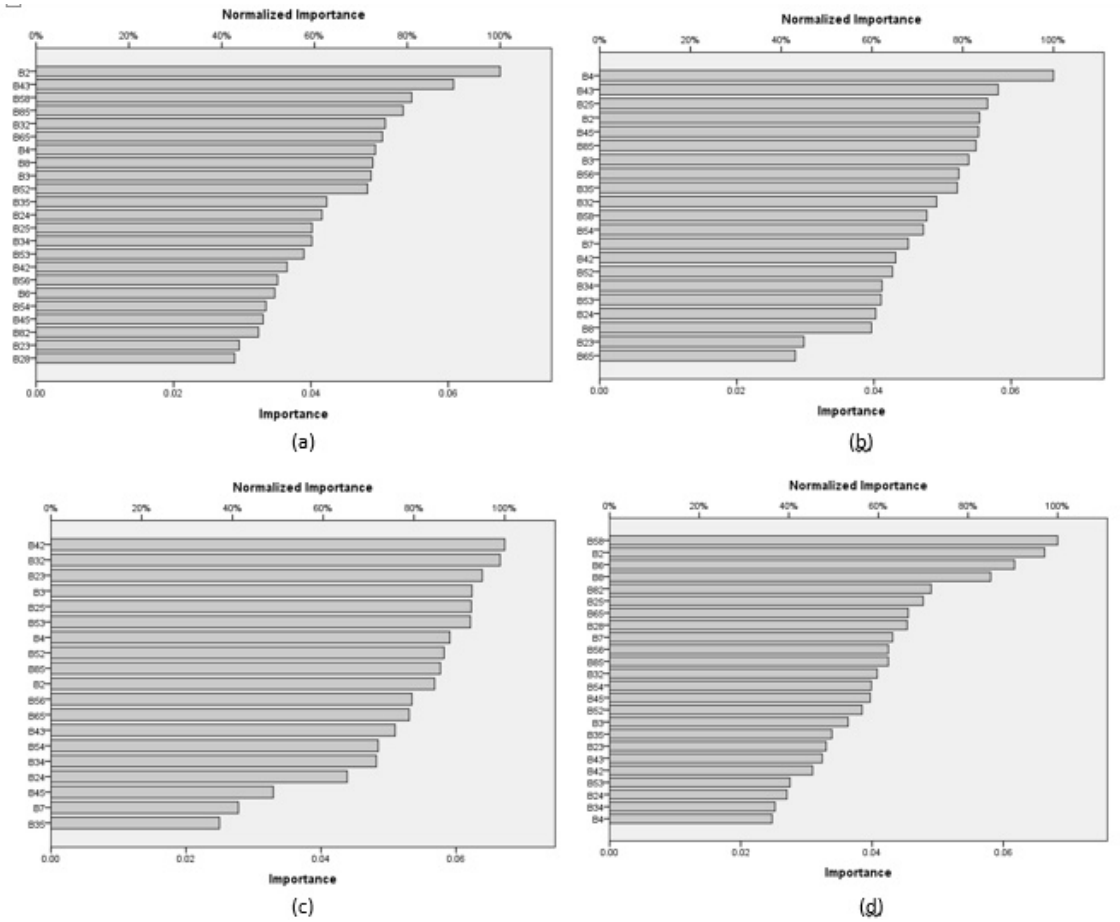

The statistical results of the developed regression models are summed up in Table 8, revealing how effectively, spatial changes in salts can be forecasted by applying different developed regression models. All of the developed regression models were immensely significant; still, models no. 3, 2, 10 and 7 were the most effective to forecast EC, pH, ESP and TSS spatial variation, respectively (Table 7), as they fulfilled all the model selection criteria. Amongst those models, model no.3, which merges B2/B4, B3/B4, B3/B5, B4/B2, and B4/B3 resulted in being the most efficient for forecasting EC. It had the highest R2 value of 0.8483, denoting a strong linear relationship amongst evaluated and forecasted EC and also made it evident that 84% of the variance in the EC values could be described by this model with comparatively low standard errors for its variables at 1.4. Each of those variables had significant p-values, implying a strong correlation with EC. In contrast, Mehrjardi et al. (2008) also discovered the red band as the most correlated with EC and based on this outcome, a regression model good enough to associate EC to red band and the exponential relation was found to be the best type of model.

Table 7: Regression Models for Different Soil Quality Parameters

Soil Quality Parameter	Model No.	MLR Equation: $Y= ß_0+ ß_1X_1+ ß_2X_2+ ß_3X_3+ ß_4X_4+ ß_5X_5$											R^2 Value	Standard Error	P-Value
		Independent Variables (Spectral Variables)					Parameters (Coefficients)								
		X_1	X_2	X_3	X_4	X_5	$ß_0$	$ß_1$	$ß_2$	$ß_3$	$ß_4$	$ß_5$			
EC	1	B4	B7	B2/B4	B3/B4	B3/B5	38.0663	-0.00017	-0.00044	-39.354	10.1769	10.8383	0.7731	1.7123	0.1229
	2	B7	B2/B4	B3/B4	B3/B5	B4/B2	-183.455	-0.00041	96.3064	-29.2337	16.0059	118.3351	0.8336	1.4662	0.0026
	3	B2/B4	B3/B4	B3/B5	B4/B2	B4/B3	-686.803	-29.5189	344.7559	20.5797	-45.9724	410.5927	0.8483	1.4001	0.0015
	4	B3/B4	B3/B5	B4/B2	B4/B3	B4/B5	51.4955	31.2349	-209.594	-10.3219	-88.4251	243.7637	0.8658	1.3169	0.8672
	5	B2	B4/B3	B5/B8	B8/B5	B3/B2	-62.8205	-0.0013	47.7298	6.430586	19.7165	13.4278	0.8043	1.5903	0.00007
	6	B4/B3	B5/B8	B8/B5	B3/B2	B6/B5	-66.3552	44.2498	7.9723	24.74293	3.2018	-1.6974	0.7942	1.6308	0.00004
	7	B5/B8	B8/B5	B3/B2	B6/B5	B4	-50.9821	7.4420	25.9168	17.80803	1.8368	0.0011	0.7339	1.8544	0.0205
	8	B8/B5	B3/B2	B6/B5	B4	B8	-49.1693	15.6043	53.0579	-0.13491	0.0015	-0.00204	0.7771	1.6973	0.0077
	9	B3	B3/B2	B5/B4	B4/B3	B4/B2	315.4758	-0.0018	-345.297	-2.34673	-316.211	375.8861	0.82231	1.5155	0.0262
	10	B2	B3	B4	B7	B8	19.9511	-0.0015	-0.0061	0.00706	-0.00036	-0.00015	0.8029	1.5959	0.0089
pH	1	B4	B4/B3	B2/B5	B2	B4/B5	8.5131	-0.0016	-2.9693	-22.6417	0.0015	29.0529	0.6961	0.3002	0.0443
	2	B4/B3	B2/B5	B2	B4/B5	B8/B5	11.2243	-4.5948	-2.6699	-0.00004	8.9576	-1.6597	0.6911	0.3026	0.0079
	3	B2/B5	B2	B4/B5	B8/B5	B3	7.5869	-0.3043	-0.00003	5.1126	-1.5515	-0.00001	0.6848	0.3058	0.0000007
	4	B2	B4/B5	B8/B5	B3	B5/B6	7.3278	-0.00008	4.9647	-1.4323	0.00002	0.0885	0.6853	0.3055	0.000009
	5	B4/B5	B8/B5	B3	B5/B6	B3/B5	6.98002	4.6516	-1.5229	-0.00002	0.0834	0.4473	0.6850	0.3056	0.00002
	6	B4/B5	B3/B5	B4/B3	B4/B2	B3/B4	101.1645	39.00362	-33.5631	-62.9459	1.9365	-34.5144	0.6808	0.3076	0.1645
	7	B3/B5	B4/B3	B4/B2	B3/B4	B5/B4	26.0620	8.2843	-12.9927	2.1864	-14.0843	1.7306	0.6753	0.3103	0.5083
	8	B4/B3	B4/B2	B3/B4	B5/B4	B5/B3	80.7989	-27.5943	2.2463	-43.0879	11.5574	-13.5867	0.6717	0.3120	0.17
	9	B4/B2	B3/B4	B5/B4	B5/B3	B2/B4	19.2943	2.8302	-13.8448	6.4747	-8.1083	3.3681	0.6658	0.3148	0.3419
	10	B3/B4	B5/B4	B5/B3	B2/B4	B4	26.3139	-14.6986	7.4751	-9.1916	0.2919	-0.00001	0.6649	0.3152	0.0017

Soil Quality Parameter	Model No.	MLR Equation: $Y= ß_0+ ß_1X_1+ ß_2X_2+ ß_3X_3+ ß_4X_4+ ß_5X_5$											R^2 Value	Standard Error	P-Value
		Independent Variables (Spectral Variables)					Parameters (Coefficients)								
		X_1	X_2	X_3	X_4	X_5	$ß_0$	$ß_1$	$ß_2$	$ß_3$	$ß_4$	$ß_5$			
ESP	1	B4/B2	B3/B2	B2/B3	B3	B2/B5	-618.948	5.9537	328.986	290.5389	-0.0005	13.0584	0.6008	1.3769	0.0906
	2	B3/B2	B2/B3	B3	B2/B5	B5/B3	-618.086	324.1847	266.2095	-0.0002	39.3916	9.1049	0.6159	1.3506	0.0851
	3	B2/B3	B3	B2/B5	B5/B3	B4	6.9766	-32.8228	-0.0008	35.9517	9.0675	0.0006	0.59	1.3954	0.808
	4	B3	B2/B5	B5/B3	B4	B5/B2	-27.0791	-0.001	33.5846	-7.7649	0.001	17.5832	0.5813	1.4101	0.3266
	5	B2/B5	B5/B3	B4	B5/B2	B8/B5	-34.4379	42.7606	-12.5205	0.0002	23.6304	-4.4881	0.5870	1.4005	0.1529
	6	B4/B5	B4/B3	B3/B5	B4/B2	B3/B4	50.9119	96.0102	-62.4014	-73.5037	3.7114	2.2146	0.6052	1.3693	0.8737
	7	B4/B3	B3/B5	B4/B2	B3/B4	B2/B4	-127.831	24.8218	15.9472	44.3103	18.5065	39.0175	0.6009	1.3768	0.5262
	8	B3/B5	B4/B2	B3/B4	B2/B4	B5/B4	-80.217	31.5911	38.6802	-12.4847	34.6425	5.1241	0.6117	1.3579	0.1478
	9	B4/B2	B3/B4	B2/B4	B5/B4	B5/B3	27.9106	27.7906	-60.0196	26.4111	33.7504	-42.2127	0.6027	1.3736	0.7516
	10	B3/B4	B2/B4	B5/B4	B5/B3	B4	95.0868	-68.7707	-2.4770	43.4199	-52.6597	-0.00004	0.5969	1.3836	0.0086
TSS	1	B5/B8	B2	B6	B8	B8/B2	-35057.9	-1526.76	3.7597	0.1831	-2.7832	30516.68	0.6102	1436.531	0.005
	2	B2	B6	B8	B8/B2	B2/B5	-32800.7	2.473041	0.132429	-1.7387	22674.67	9172.511	0.6448	1371.285	0.005
	3	B6	B8	B8/B2	B2/B5	B6/B5	-12705.8	0.0648	0.4828	3879.774	12214.02	-172.261	0.6152	1427.225	0.0031
	4	B8	B8/B2	B2/B5	B6/B5	B2/B8	-71134.3	0.6591	31702.13	11147.62	1188.619	29087.35	0.62	1418.32	0.3548
	5	B8/B2	B2/B5	B6/B5	B2/B8	B7	-110246	53449.59	8681.711	-680.348	49958.73	0.5528	0.7186	1220.546	0.0988
	6	B4/B3	B4/B2	B4/B5	B3/B4	B2/B4	-398913	233902.6	-26812.7	14423.63	203373.4	-16840.7	0.8512	887.4046	0.0024
	7	B4/B2	B4/B5	B3/B4	B2/B4	B4	-131168	85711.9	13435.16	-6962.76	60136.75	-1.1971	0.8557	873.8704	0.0002
	8	B4/B5	B3/B4	B2/B4	B4	B7	10322.99	11719.83	19877.59	-27226.6	-0.1628	-0.2845	0.7890	1056.722	0.5402
	9	B3/B4	B2/B4	B4	B7	B3/B5	24362.43	6513.263	-25186.6	-0.1076	-0.28191	6936.533	0.77315	1095.901	0.1229
	10	B2/B4	B4	B7	B3/B5	B5/B4	-5302.51	-30669.2	-0.0594	-0.4606	46456.37	11062.66	0.8415	915.82	0.7024

Contrarily, model no.2, which merges B4/B3, B2/B5, B2, B4/B5, and B8/B5 provided the best fit for predicting pH of the soil with the R^2 value of 0.69 and relatively low standard errors of 0.3. Similarly, model no.10, which combines B3/B4, B2/B4, B5/B4, B5/B3 and B4, and model no.7, which combines B4/B2, B4/B5, B3/B4, B2/B4, and B4 provided the best fit for predicting ESP and TSS respectively with the R^2 value of 0.59 and 0.85.

Model Validation and Generation of Maps

The effectiveness of the developed regression models on the data of 2014 was quantified using the ground truth data of fifty (50) sampling points and image of 2016. The justification of 50 sampling points derived from exploring the terrain, and from recommendations and practices from similar studies relying on remote sensing (Galvao *et. al.,* 2008). Samples were collected from agricultural fields, which were severely affected by the salts, with the help of the farmers working there. The west side of the study area was not sampled, as the block of the district was completely urbanized.

Figure 6 presents the validation outcomes for the finest regression models. Selected models perform well with respect to the normality test of the residuals. Moreover, the W test for model 3 for EC upgraded to 0.87 with a non-significant *p*-value ($p < 0.05$), presents a normal distribution of the residuals. Also, the values of R^2 equaling 0.765 and RMSE of 1.56 dS/m reveal that this regression model is the most efficient for predicting EC as compared to the others. The selected model for predicting EC in this study seems to outweigh in the prediction power ($R^2 = 0.76$) of soil salinity over those described by Shrestha in 2006 with R^2 equal to 0.23, Shamsi *et al.* in 2013 with R^2 equal to 0.39 and Allbed *et. al.* in 2014 with R^2 value equal to 0.65, using different moderate resolution images. Nevertheless, dissimilarity in spatial resolution can have a significant influence on forecasting soil salinity (Figure 6).

Values of R^2 and RMSE as 0.268 and 0.5, respectively, for the regression model no. 2 of pH showed that this model would not ascertain soil sodicity with high precision making use of remotely sensed data. As per validation outcomes for ESP and TSS models, the W-test for model 10 for ESP improved to 0.93 with an insignificant *p*-value of 0.01, indicating the normal distribution of the residuals. Moreover, the values of R^2 equaling 0.46 and RMSE of 1.45 indicate that this regression model is appropriate for predicting ESP. Furthermore, W-test statistic value of 0.78 for model no. Ten for TSS and R^2 of 0.53 indicate the normal distribution of the residuals, as well as the model, is the best fit for predicting TSS. Hence, those statistical outcomes indicate that the regression model no. 3 for EC, model no. Ten for ESP and model no. Seven for TSS meet both the model selection as well as the model evaluation criteria. As a result, the best-executed regression model that fulfilled all the model selection and validation principles were selected and put in use to forecast and map the spatial changes in soil salinity. Each one of the statistical analysis was undertaken in SPSS 20, with significance levels set to $p < 0.05$.

Fig. 6: Validation results for the best regression models

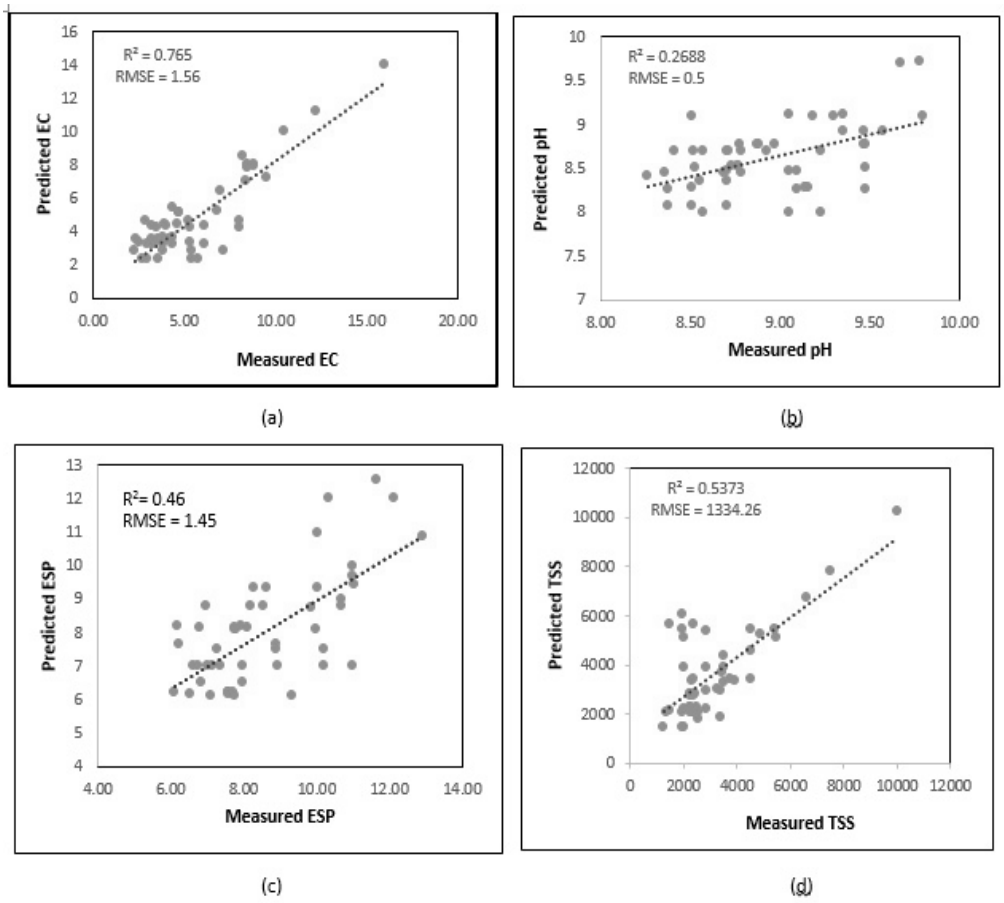

In addition to statistical tests, the data enabled us to generate soil parameter maps of the area of interest for each of the chosen models. The benefit of these maps is that they visualize the locations and distributions of the saline and sodic areas in relation to those where agriculture is practiced. Most of the agricultural land in the study area is moderately saline (EC = 3-6 dS/m) and moderately sodic (pH = 8.48-8.69) soil. ESP is one more parameter that symbolizes soil sodicity. As per the ESP simulation map, the range of ESP in our study area is 6.83-7.53, which shows that our study area is not facing problems due to excess sodium. Furthermore, the result showed that there exists a linear relationship between EC and TSS within a certain range, which can be useful in estimating soluble salts in a soil sample. The range of TSS in the present study throughout the study area is 1073-2194 mg/l, which shows that the concentration of the soluble salts is towards the higher side.

As observed, a lower concentration of salt accumulation in the vegetated areas may be due to the fact that, vegetated regions are exposed to a leaching process which lowers salt levels. Still, there is a significant variation in salt over the vegetated areas throughout the study area. These differences are considered mainly caused by poor drainage and improper irrigation management.

Soil Degradation Probability Map using Analytical Hierarchy Process

The overall map showing soil degradation probability zone was generated by overlaying different maps (EC, pH, TSS, ESP, NDSI, and NDVI) using GIS integration. Weights for each soil salinity criteria were calculated using AHP (Table no. 8), with the CR value equal to 0.09. According to which the highest weight was assigned to NDSI (0.266) and the least weight was assigned to ESP (0.092).

Table 8: Weighted Linear Combination (WLC)

S.No.	Layer Name	Weights
1	NDSI	0.266
2	TSS	0.213
3	EC	0.165
4	NDVI	0.16
5	ESP	0.092
6	pH	0.104

The soil degradation probability zones compared to soil salinity and sodicity in the study area have been classified into five classes viz., least, low, moderate, high and very high susceptibility towards salt. According to the final simulated map of the soil quality of the district, major portion of the total agricultural land of the study area lie between low (32.74 %) to moderate (29.53 %) probability zones of salt susceptibility, whereas 22.78 % of the total cropland has the least susceptibility to salt. 5.66% and 9.26% of the agricultural land of the study area is liable to high and very high probability of getting degraded due to salt-affected soil, respectively (Table 9, Figure 7).

Table 9: Area of Soil Degradation Probability Zones

Class	Probability Zones	Area (sq km)	% Area
1	Least	168.128	22.78
2	Low	241.569	32.74
3	Moderate	217.877	29.53
4	High	41.815	5.66
5	Very High	68.371	9.26
Total		**737.76**	**100**

Fig. 7: Soil degradation probability zones

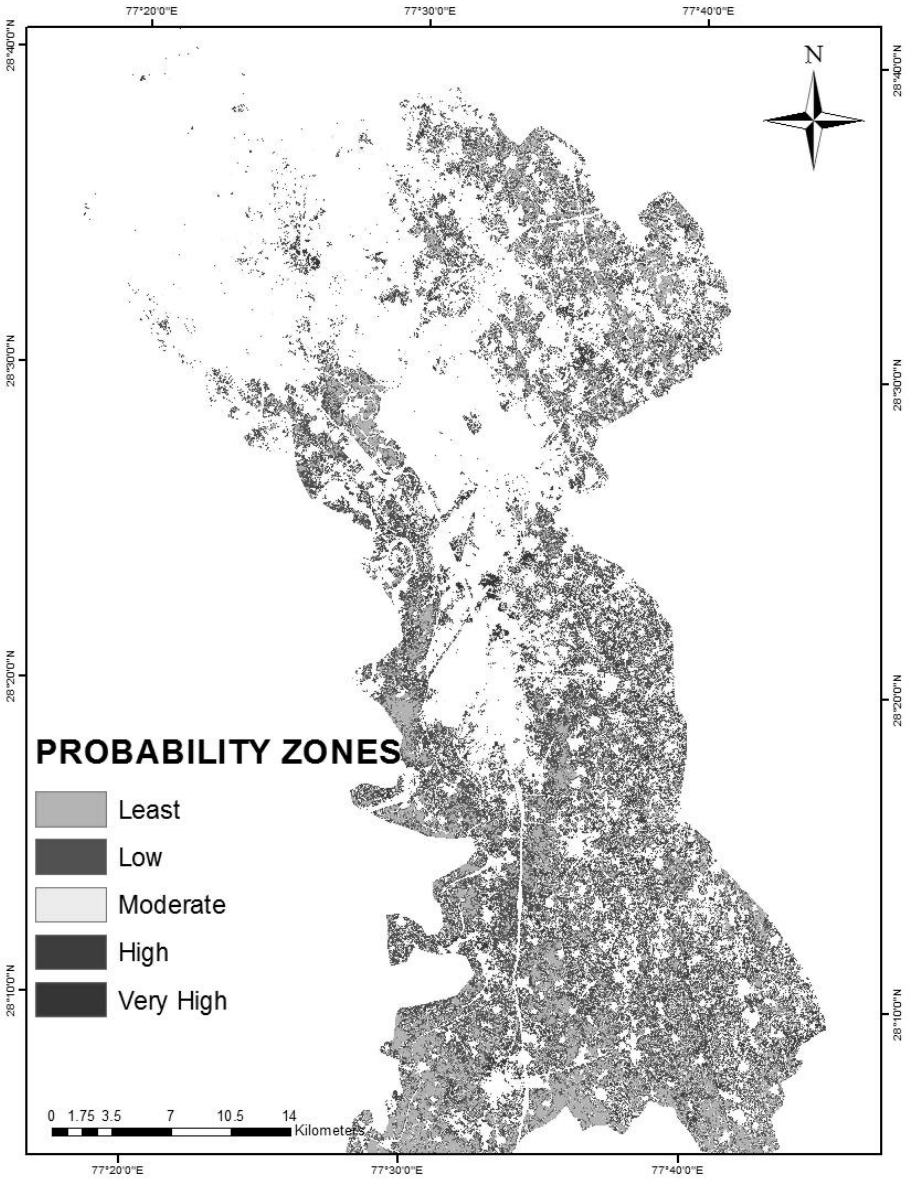

CONCLUSION

Responding to the key objectives of our research, we concluded that it is possible to understand the characteristics of salt affected soil with the spectral reflectance. The harmony between satellite driven data and on-field data can be used in the future and greater correlation can be witnessed. We further conclude that Landsat-8 (OLI & TIRS) satellite data cannot be put in use for the estimation of SAR of the soil as all the bands and ratios

showed a non-significant correlation with field analyzed SAR data. We also put forward that Blue, Green, Red & NIR bands of Landsat-8 (OLI & TIRS) are the most suitable bands for the study of salt affected and degraded soil. Through our study, it is evident that the ANN followed by MLR is an effective statistical tool for the assessment of the relation between field measurements and the satellite imagery through models. Further, the AHP method is most appropriate for assigning weights to all the soil quality parameters and indices for the generation of soil degradation probability zone map. After analyzing the soil degradation probability zone map generated using spatio-temporal model, we concluded that most of the part of the study area lies under low and moderate soil degradation probability zones, and very less part of the area lies under high and very high impact zones respectively, which clearly states that there is hardly any unaffected area left.

Finally, we summarize that random sample surveys in farmlands, including soil quality, provide an interesting tool to assess the effects of proposed land improvement projects. This study also reveals how statistical analysis, paired with satellite images of high spatial resolution, could efficiently forecast and map spatial changes in soil quality across agricultural land. Therefore, the information dispensed here can assist agricultural workers, scientists and engineers in controlling soil related troubles influencing the environment. Also, the straightforwardness of this approach, with its adequate correctness, can impart considerably to soil salinity and sodicity prediction and mapping, in more economical ways than conventional approaches. It will be valuable information for policy and decision makers for sustainable land resource development with respect to food security and crop productivity.

REFERENCES

Abrol, A.P. and Bhumbla, D. R. (1971). Saline and alkali soils in India- their occurrence and management. *World Soil Resources Report*. 41-42.

Afework, M. (2009). *Analysis and Mapping of Soil Salinity Levels in Metehara Sugarcane Estate Irrigation Farm Using Different Models*. Ms.C. Thesis, Addis Ababa University, Ethiopia, Addis Ababa.

Akramkhanov, A., C. Martius, S. J. Park and J. M. H. Hendrickx. (2011). Environmental factors of spatial distribution of soil salinity on flat irrigated terrain.*Geoderma*, 163(1-2), 55-62.

Akramkhanov, A.; Vlek, P. (2012). The assessment of spatial distribution of soil salinity risk using neural network. *Environ. Monit. Assess.*, *184*, 2475–2485.

Allbed A., Kumar L. and Sinha P. (2014). Mapping and Modelling Spatial Variation in Soil Salinity in the Al Hassa Oasis Based on Remote Sensing Indicators and Regression Techniques. *Remote Sens*, *6*, 1137-1157; doi:10.3390/rs6021137.

Azabdaftari, A., Sunarb, F. (2016). Soil Salinity Mapping using Multitemporal Landsat Data. In *The International Archives of the Photogrammetry, Remote Sensing and Spatial Information Sciences (*p. 80-122), Volume XLI-B7, 2016, XXIII ISPRS Congress, 12–19 July 2016, Prague, Czech Republic.

Bannari, A. M. Guedona, A. El-Hartib, F. Z. Cherkaouic and A. El-Ghmari, (2008). Characterization of Slightly and Mo- derately Saline and Sodic Soils in Irrigated Agricultural Land using Simulated Data of Advanced Land Imaging (EO-1) Sensor,*Communications in Soil Science and Plant Analysis*, Vol. 39 (19), 2795-2811.

Bouaziz, M.; Matschullat, J.; Gloaguen, R. (2011). Improved remote sensing detection of soil

salinity from a semi-arid climate in Northeast Brazil. *ComptesRendusGeosci.*, *343*, 795–803.

Campbell, J.B. (2002). Introduction to Remote Sensing, *Published by Taylor and Francis, London and New York (First Indian Reprint 2003, printed at Chennai Micro Print Pvt. Ltd., Chennai)*, 621.

Cozzolino D, Moron A. (2003). The potential of near-infrared reflectance spectroscopy to analyse soil chemical and physical characteristics. *Journal of Agricultural Sciences* 140: 65-71.

Douaik, A.; van Meirvenne, M.; Toth, T.; Serre, M. (2004). Space-time mapping of soil salinity using probabilistic bayesian maximum entropy. *Stoch. Environ. Res. Risk Assess.*, *18*, 219–227.

Elnaggar and Noller, J.S., (2009). Application of Remote- Sensing Data and Decision-Tree Analysis to Mapping Salt- Affected Soils over Large Areas, *Remote Sensing*, 2 (1): 151-165. http://dx.doi.org/10.3390/rs2010151

Fan X., Pedroli, B; Liu G, Liu Q, Liu H and Shu L. (2012). Soil Salinity Development in the Yellow River Delta in Relation to Groundwater Dynamics,*Land Degradation & Development*, 23(2), 175-189.

Farifteh, J., A. Farshad and R. George. (2006). Assessing salt-affected soils using remote sensing, solute modelling, and geophysics.*Geoderma 130*(3): 191-206.

Fernandez-Buces, N.; Siebe, C.; Cram, S. and Palacio, J., (2006). Mapping soil salinity using a combined spectral response index for bare soil and vegetation: A case study in the former lake Texcoco, Mexico. *J. Arid Environ. 65*, 644–667.

Fernandez-Buces, N.; Siebe, C.; Cram, S.; Palacio, J. (2006). Mapping soil salinity using a combined spectral response index for bare soil and vegetation: A case study in the former lake Texcoco, Mexico. *J. Arid Environ.*, *65*, 644–667.

Field, A.; Miles, J.; Field, Z. (2012). *Discovering Statistics Using R*; SAGE Publications: London, UK; 992.

Galvao. L.S., Formaggio, A.R., Couto, E.G. & Roberts, D.A. (2008). Relationship between the mineralogical and chemical composition of tropical soils and topography from hyperspectral remote sensing data. *ISPRS Journal of Photogrammetry and Remote Sensing*, 63 (2): 259-271.

Girard, M.C. and Girard, C. (2003). Processing of Remote Sensing Data, *Translated by N. Venkat Rao, Oxford & IBH Publishing Co. Pvt. Ltd., New Delhi, Publications*, pp. 486

IDNP, (2003). *Indo Dutch Network Project: A Methodology for identification of Waterlogging Soil salinity conditions using remote sensing*. Central soil Salinity Research Institute, Karnal, India 78 pages.

Jabbar M.T., and Chen. X., (2008). Land Degradation Due to Salinization in Arid and Semi-Arid Regions with the Aid of Geo-Information Techniques, *Geo-Spatial Information Science*, 11(2), 112-120. http://dx.doi.org/10.1007/s11806-008-0013-z

Janik LJ, Forrester ST, Rawson A. (2009). The prediction of soil chemical and physical properties from mid-infrared spectroscopy and combined partial-least squares regression and neural networks (PLS-NN) analysis. *Chemometrics and Intelligent Laboratory Systems* 97: 179- 188.

Jian-li D, Man-chun W, Tiyip T. (2011). Study on soil salinization information in arid region using remote sensing technique. *Agricultural Sciences in China* 10: 404-411.

Judkins, G.; Myint, S. (2012). Spatial variation of soil salinity in the Mexicali valley, Mexico: Application of a practical method for agricultural monitoring. *Environ. Manag., 50*, 478–48..

Kant, Y., Nigam, R.K. and Jayanti, S.C. (1997). Change Detection of Micro Level for Landuse/ Landcover Using Remote Sensing Data, *Symposium of Remote Sensing for Natural Resources with Special Emphasis on Infrastructure Development* held at NRSA, Hyderabad from November 26-28, 1997. A Joint ISRS, Dehradun and NNRMS, Bangalore Publication (Eds: Rabindran, K.V., Prasad, J., Pande, L.M., Kushwaha, S.P.S. and Saha, S.K.)Remote Sensing and Geographical Information System for Natural resources,pp. 65-74

Khan, N.M., Rastoskuev, V.V., Sato, Y. and Shiozawa, S., (2005). Assessment of Hydrosaline Land Degradation by Using a Simple Approach of Remote Sensing Indicators, *Agricultural Water Management*, 77(1), 96-109. http://dx.doi.org/10.1016/ j.agwat.2004.09.038.

Knipling E.B. (1970). Physical and Physiological Bases for the Reflectance of Visible and near Infrared from Vegetation, *Remote Sensing of Environment*, 1:155-159.

Mehrjardi, R.T.; Mahmoodi, S.H.; Taze, M.; Sahebjalal, E (2008). Accuracy assessment of soil salinity map in Yazd-Ardakan Plain, Central Iran, based on Landsat ETM+ imagery. *Am.-Eurasian J.Agric. Environ. Sci., 3*, 708–712.

Mehrjardi, R.T.; Minasny, B.; Sarmadian, F.; Malone, B. (2014). Digital mapping of soil salinity in Ardakan region, central Iran. *Geoderma, 213*, 15–28.

Metternicht, G.; Zinck, A. (2008). *Remote Sensing of Soil Salinization: Impact on Land Management*; CRC Press: Boca Raton, FL, USA; 377.

Moriasi, D.; Arnold, J.; van Liew, M.; Bingner, R.; Harmel, R.; Veith, T. (2007). Model evaluation guidelines for systematic quantification of accuracy in watershed simulations. *Trans. ASABE, 50*, 885–900.

Norman C.P, Lyle C.W. Heuperman A.F. and Poulton D. (1989). Tragowel Plains – Challenge of the plains: In *Tragowel Plains Salinity Management Plan, Soil salinity survey, Tragowel plains subregional working group* (pp. 49-89). Melbourne: Victorian, Department of Agriculture.

Patel AD, Bhensdadia H, Pandey AN. (2009). Effect of salinization of soil on growth, water status and general nutrient accumulation in seedlings of Delonisregia (Fabaceae). *Acta EclogicaSinica* 29: 109-115.

Pérez González M. E., Rodríguez M. P. G., González-Quiñones V. and Jiménez Ballesta, R. (2006). Spatial Va- riability of Soil Quality in the Surroundings of a Saline Lake Environment, *Environmental Geology*, 51 (1), 143-149. http://dx.doi.org/10.1007/ s00254-006-0317-y

Ramanathan R. (2001). A note on the use of the analytic hierarchy process for environmental impact assessment, *Journal of EnvironmentalManagement*, 63, 27-35.

Richards L. (1954). Diagnosis and Improvement of Saline and alkali Soils, *Soil Science*, 78 (2), 154.Richards, L. Determination of the Properties of Saline and Alkali Soils. In *Diagnosis and Improvement of Saline and Alkali Soils, Agriculture Handbook No. 60*; US Regional SalinityLaboratory: Riverside, CA, USA, 1954; pp. 7–33.

Saaty T.L. (1977). A scaling method for priorities in hierarchical structures, *Journal ofMathematical Psychology*, 15, 234–281.

Saaty T.L. (1980). *The analytic hierarchy process: planning, priority setting, resource allocation.* McGraw-Hill International Book Company,New York.

Saaty T.L. (2000). *Fundamentals of decision making and priority theory with the Analytic Hierarchy Process*, RWS Publications, Pittsburg.

Selch, D. (2012). Comparing salinity models in Whitewater Bay using remote sensing, *Florida Atlantic University*.

Shamsi, F.R.S.; Sanaz, Z.; Abtahi, A.S. (2013). Soil salinity characteristics using moderate resolution imaging spectroradiometer (MODIS) images and statistical analysis. *Arch. Agron. Soil Sci.59*, 471–489.

Shrestha, R. (2006). Relating soil electrical conductivity to remote sensing and other soil properties for assessing soil salinity in northeast Thailand. *Land Degrad. Dev.17*, 677–689.

Somvanshi S, Kunwar P., Singh N. B, Shukla S.P and Pathak V. (2012). Integrated Remote Sensing and GIS for Water Quality Analysis of Gomti River, Uttar Pradesh, *International Journal of Environmental Sciences,* 3 (1): 62-74.

Somvanshi S.S, Kunwar P, Tomar S, Singh M, (2017). Comparative Statistical Analysis of the Quality of Image Enhancement Techniques, *International Journal of Image and Data Fusion.* DOI – 10.1080/19479832.2017.1355336

Tajgardan, T.; Shataee, S.; Ayoubi, S. (2007). In Spatial Prediction of Soil Salinity in the Arid Zones Using ASTER Data, Case study: North of Ag Ghala, Golestan Province, Iran. In *Proceedings of Asian Conference on Remote Sensing (ACRS*) (pp. 5-10), Kuala Lumpur, Malaysia, 12–16 November 2007.